consumption varies continuously with the level of AGRP neuron activation, nearly full suppression of activity is required to block the evoked feeding response (*28*).

AGRP neurons in *Agrp-cre* mice (*29*) were transduced using a bicistronic Cre recombinase (Cre)–dependent viral vector (*30*) (Fig. 4A). AGRP neurons coexpressing ChR2 and PSAM^{L141F,Y115F}-GlyR (Fig. 4B) could be activated with light and were reversibly silenced by PSEM^{89S} during photostimulation in brain slices (Fig. 4, C and D). Mice coexpressing ChR2 and PSAM^{L141F,Y115F}-GlyR or expressing ChR2 alone in AGRP neurons ate voraciously in response to photostimulation after intraperitoneal (i.p.) saline injection, and, for each mouse, this consumption was used as the baseline for subsequent treatments. After i.p. administration of PSEM^{89S}, photostimulation-evoked feeding was strongly suppressed in mice expressing PSAM^{L141F,Y115F}-GlyR but not in mice expressing only ChR2 (Fig. 4, E and F). Twenty-four hours later, photostimulation-evoked food intake recovered to baseline levels (two-way analysis of variance, one-factor repeated measure, ±PSEM^{89S}: $F_{1,9} = 12.9$, $P = 0.006$; ±PSAM^{L141F,Y115F}-GlyR: $F_{1,9} = 1.3$, $P = 0.30$; interaction: $F_{1,9} = 22.4$, $P < 0.001$; Fig. 4, E and F). Moreover, after photostimulation, Fos, a marker of neuron activation (*31*), was almost completely suppressed in ChR2-expressing neurons from mice administered PSEM^{89S} (fig. S14). Thus, PSAM^{L141F,Y115F}-GlyR and PSEM^{89S} constitute an effective neuronal silencer system in vivo, even for strong, synchronous depolarizing currents that result from ChR2 photoactivation.

Our results show how concerted chemical and genetic engineering of a complex ligand-binding interface can be used to develop pharmacologically selective actuators and small-molecule effectors for construction of a LGIC toolbox. PSEMs, the agonists for the resulting ion channels, act rapidly in the brain after peripheral delivery. Together, these components enable combinatorial construction (fig. S15) of cell type–selective tools to control a range of conductances, which can be used to activate or silence neurons. These ion channels could be further elaborated by applying extensive structure-function relationships in Cys-loop receptors, including mutations that modify ion selectivity (*27*, *32*–*34*), intracellular interactions (*35*–*37*), and desensitization (*27*, *38*, *39*). The pharmacologically orthogonal ion channels described here can also be used with each other or with existing tools such as channelrhodopsin, facilitating multiple perturbations in the same organism to investigate functions of ion flux in cell biology, physiology, and behavior.

References and Notes

1. E. M. Slimko, S. McKinney, D. J. Anderson, N. Davidson, H. A. Lester, *J. Neurosci.* **22**, 7373 (2002).
2. E. M. Tan *et al.*, *Neuron* **51**, 157 (2006).
3. P. Wulff *et al.*, *Nat. Neurosci.* **10**, 923 (2007).
4. B. N. Armbruster, X. Li, M. H. Pausch, S. Herlitze, B. L. Roth, *Proc. Natl. Acad. Sci. U.S.A.* **104**, 5163 (2007).
5. S. Gosgnach *et al.*, *Nature* **440**, 215 (2006).
6. W. Lerchner *et al.*, *Neuron* **54**, 35 (2007).
7. S. M. Ferguson *et al.*, *Nat. Neurosci.* **14**, 22 (2011).
8. E. S. Boyden, F. Zhang, E. Bamberg, G. Nagel, K. Deisseroth, *Nat. Neurosci.* **8**, 1263 (2005).
9. X. Li *et al.*, *Proc. Natl. Acad. Sci. U.S.A.* **102**, 17816 (2005).
10. F. Zhang *et al.*, *Nature* **446**, 633 (2007).
11. J. L. Eiselé *et al.*, *Nature* **366**, 479 (1993).
12. T. Grutter *et al.*, *Proc. Natl. Acad. Sci. U.S.A.* **102**, 18207 (2005).
13. H. A. Lester, M. I. Dibas, D. S. Dahan, J. F. Leite, D. A. Dougherty, *Trends Neurosci.* **27**, 329 (2004).
14. J. A. Dent, *J. Mol. Evol.* **62**, 523 (2006).
15. A. Tasneem, L. M. Iyer, E. Jakobsson, L. Aravind, *Genome Biol.* **6**, R4 (2005).
16. Y. W. Hwang, D. L. Miller, *J. Biol. Chem.* **262**, 13081 (1987).
17. A. C. Bishop *et al.*, *Nature* **407**, 395 (2000).
18. Q. Lin, F. Jiang, P. G. Schultz, N. S. Gray, *J. Am. Chem. Soc.* **123**, 11608 (2001).
19. P. H. Celie *et al.*, *Neuron* **41**, 907 (2004).
20. D. P. Walker *et al.*, *Bioorg. Med. Chem.* **14**, 8219 (2006).
21. A. L. Bodnar *et al.*, *J. Med. Chem.* **48**, 905 (2005).
22. P. N. Vinson, J. B. Justice Jr., *J. Neurosci. Methods* **73**, 61 (1997).
23. J. L. Galzi *et al.*, *FEBS Lett.* **294**, 198 (1991).
24. S. P. Kelley, J. I. Dunlop, E. F. Kirkness, J. J. Lambert, J. A. Peters, *Nature* **424**, 321 (2003).
25. D. Rayes, G. Spitzmaul, S. M. Sine, C. Bouzat, *Mol. Pharmacol.* **68**, 1475 (2005).
26. P. Séguéla, J. Wadiche, K. Dineley-Miller, J. A. Dani, J. W. Patrick, *J. Neurosci.* **13**, 596 (1993).
27. J. L. Galzi *et al.*, *Nature* **359**, 500 (1992).
28. Y. Aponte, D. Atasoy, S. M. Sternson, *Nat. Neurosci.* **14**, 351 (2011).
29. C. B. Kaelin, A. W. Xu, X. Y. Lu, G. S. Barsh, *Endocrinology* **145**, 5798 (2004).
30. D. Atasoy, Y. Aponte, H. H. Su, S. M. Sternson, *J. Neurosci.* **28**, 7025 (2008).
31. J. I. Morgan, T. Curran, *Annu. Rev. Neurosci.* **14**, 421 (1991).
32. D. Bertrand, J. L. Galzi, A. Devillers-Thiéry, S. Bertrand, J. P. Changeux, *Proc. Natl. Acad. Sci. U.S.A.* **90**, 6971 (1993).
33. A. Keramidas, A. J. Moorhouse, C. R. French, P. R. Schofield, P. H. Barry, *Biophys. J.* **79**, 247 (2000).
34. M. J. Gunthorpe, S. C. Lummis, *J. Biol. Chem.* **276**, 10977 (2001).
35. M. K. Temburni, R. C. Blitzblau, M. H. Jacob, *J. Physiol.* **525**, 21 (2000).
36. J. Xu, Y. Zhu, S. F. Heinemann, *J. Neurosci.* **26**, 9780 (2006).
37. M. Jansen, M. Bali, M. H. Akabas, *J. Gen. Physiol.* **131**, 137 (2008).
38. F. Revah *et al.*, *Nature* **353**, 846 (1991).
39. H. G. Breitinger, C. Villmann, K. Becker, C. M. Becker, *J. Biol. Chem.* **276**, 29657 (2001).

Acknowledgments: Supported by the Howard Hughes Medical Institute. C.J.M. performed the electrophysiology and the imaging; P.H.L. synthesized the molecules and performed the MP screen; D.A. performed the behavioral experiments; H.H.S. made the mutant channels and other constructs; L.L.L. made the homology model; and S.M.S. developed the mutant ion channel screen, planned the experiments, analyzed data, and wrote the paper with comments from all authors. We thank S. Winfrey and H. White for cell culture support. S.M.S., P.H.L., and L.L.L. are inventors on a patent application by the Howard Hughes Medical Institute regarding combined use of these ligand-gated ion channels and small-molecule agonists.

Supporting Online Material

www.sciencemag.org/cgi/content/full/333/6047/1292/DC1
Materials and Methods
Figs. S1 to S15
Tables S1 to S3
Movie S1
References (*40*–*42*)

6 April 2011; accepted 8 August 2011
10.1126/science.1206606

Potential for Chemolithoautotrophy Among Ubiquitous Bacteria Lineages in the Dark Ocean

Brandon K. Swan,[1] Manuel Martinez-Garcia,[1] Christina M. Preston,[2] Alexander Sczyrba,[3] Tanja Woyke,[3] Dominique Lamy,[4]* Thomas Reinthaler,[4] Nicole J. Poulton,[1] E. Dashiell P. Masland,[1] Monica Lluesma Gomez,[1] Michael E. Sieracki,[1] Edward F. DeLong,[5] Gerhard J. Herndl,[4] Ramunas Stepanauskas[1]†

Recent studies suggest that unidentified prokaryotes fix inorganic carbon at globally significant rates in the immense dark ocean. Using single-cell sorting and whole-genome amplification of prokaryotes from two subtropical gyres, we obtained genomic DNA from 738 cells representing most cosmopolitan lineages. Multiple cells of *Deltaproteobacteria* cluster SAR324, *Gammaproteobacteria* clusters ARCTIC96BD-19 and Agg47, and some *Oceanospirillales* from the lower mesopelagic contained ribulose-1,5-bisphosphate carboxylase-oxygenase and sulfur oxidation genes. These results corroborated community DNA and RNA profiling from diverse geographic regions. The SAR324 genomes also suggested C_1 metabolism and a particle-associated life-style. Microautoradiography and fluorescence in situ hybridization confirmed bicarbonate uptake and particle association of SAR324 cells. Our study suggests potential chemolithoautotrophy in several uncultured *Proteobacteria* lineages that are ubiquitous in the dark oxygenated ocean and provides new perspective on carbon cycling in the ocean's largest habitat.

The dark ocean (below 200 m) contains an active and metabolically diverse microbial assemblage that is responsible for the majority of marine organic carbon mineralization (*1*). In addition to heterotrophic microbial activity, autotrophic carbon assimilation may be significant not only in oxygen minimum zones (OMZs) and anoxic basins (*2*–*4*), but also

throughout the oxygenated water column (*5*–*7*). In the North Atlantic, the dark ocean's primary production is 20 to 40% of the photic zone's exported production and may be of the same order of magnitude as the dark ocean's heterotrophic production (*6*). It has been generally assumed that the predominant type of autotrophy in the dark ocean is CO_2 fixation through the 3-hydroxypropionate/4-hydroxybutyrate cycle, driven by the archaeal marine group I *Crenarchaea* and fueled by ammonia oxidation (*8*, *9*). However, archaeal nitrification may be insufficient to support the measured inorganic carbon fixation rates in some regions of the North Atlantic (*6*, *10*, *11*). Thus, as yet unidentified microbial lineages and energy sources may be responsible for a significant fraction of carbon fixation in the dark ocean. The paucity of representative pure cultures has hindered experimental and genomic studies of the majority of bacterioplankton from the deep ocean so far.

We used single-cell sorting and DNA sequencing to identify the predominant bacterial lineages in the mesopelagic that contain genes for inorganic carbon fixation (*12*). This approach can link phylogenetic [such as small subunit ribosomal RNA (SSU rRNA)] and metabolic marker genes by sequencing them from the same cell obtained directly from its environment, without the need for cultivation (*13*–*17*). Using single-cell sorting and whole-genome amplification, we generated libraries of prokaryotic single amplified genomes (SAGs) from surface and mesopelagic samples from the South Atlantic and North Pacific Subtropical Gyres (figs. S1 and S2). By polymerase chain reaction (PCR) and subsequent sequencing of the SSU rRNA genes, we identified 502 mesopelagic and 236 surface-ocean prokaryote SAGs (Fig. 1 and Table 1). Microbial community composition, as determined by SAG libraries, differed between the surface and the mesopelagic zones within each gyre. In contrast, microbial composition was similar between samples collected at similar depths at the two stations, especially for the mesopelagic (Fig. 1), in agreement with past studies employing more traditional molecular techniques (*18*, *19*). Overall, our SAG libraries captured the majority of previously described uncultivated marine lineages and opened the door for their genomic study (Fig. 1 and figs. S3 to S11).

Using PCR, we screened mesopelagic SAGs for several key genes mediating carbon fixation and chemolithotrophic energy production (table S1) and found that *Deltaproteobacteria* cluster SAR324, *Gammaproteobacteria* clusters ARCTIC96BD-19 and Agg47, and some *Oceanospirillales* possess genes for both carbon fixation and sulfur oxidation (Fig. 2). PCR did not detect genes central to the reductive tricarboxylic acid cycle. However, sequences (*cbbL and cbbM*) coding for the large subunit of ribulose-1,5-bisphosphate carboxylase-oxygenase (RuBisCO), a key enzyme mediating the Calvin-Benson-Bassham (CBB) cycle, were recovered from 47% of SAR324 (the first record of RuBisCO in *Deltaproteobacteria*), 25% of *Gammaproteobacteria*, and 12% of all mesopelagic bacteria SAGs. These gene frequencies represent minimal estimates and may be higher within the bacterioplankton. Several inherent limitations in the PCR-based SAG screening approach applied here could lead to an underestimation of these frequencies, including incomplete whole-genome amplification, PCR primer mismatches, and PCR template secondary structures. For comparison, *rec*A-normalized abundances of RuBisCO genes recovered from several dark ocean (≥500 m) metagenomes and a metatranscriptome at station ALOHA were 6 to 26% and 33%, respectively (table S2). Together, SAR324, ARCTIC96BD-19, Agg47, and *Oceanospirillales* made up 31 and 34% of all bacterial SAGs from the South Atlantic and North Pacific mesopelagic, respectively. This is consistent with previous findings of high abundances of these lineages in the dark ocean in various geographic regions (*18*, *20*, *21*), which is indicative of their significance in biogeochemical processes.

Genomic sequencing of two ARCTIC96BD-19 and two SAR324 SAGs (tables S7 to S9) recovered complete RuBisCO operons in all four SAGs (tables S10 to S13). Phylogenetic analysis of gene sequences and the presence of protein active sites, RuBP binding sites, and RuBisCO sequence motifs confirm that these are bona fide RuBisCO genes, in contrast to RuBisCO-like systems found in certain bacteria and archaea (fig. S12 and S13) (*22*). Nonfunctional genes are rare in oligotrophic bacterioplankton (*23*, *24*). Thus, the presence of RuBisCO genes in the mesopelagic is likely to be indicative of carbon fixation via the CBB cycle by several indigenous bacterial lineages and could account for at least some of the RuBisCO proteins observed below the photic zone (*25*). A closely related cDNA sequence from 500 m at station ALOHA (*26*) provides evidence for RuBisCO gene expression in situ (fig. S12). Microautoradiography linked with catalyzed reporter deposition fluorescence in situ hybridization (MAR-CARD-FISH) performed on prokaryotes from an oceanic station in the North Atlantic (fig. S1) confirmed that at least one of the RuBisCO-containing groups, SAR324, assimilated inorganic carbon in situ (Fig. 3, A and B). The SAR324 cells constituted 6 to 17% of all prokaryotes, and 3 to 21% of SAR324 cells exhibited detectable bicarbonate assimilation throughout the meso- and bathypelagic (Fig. 3C). The bicarbonate-active SAR324 cells made up 20.4 ± 13.3% (n = 5 samples) of total bicarbonate-positive 4′,6-diamidino-2-phenylindole–stained cells, suggesting

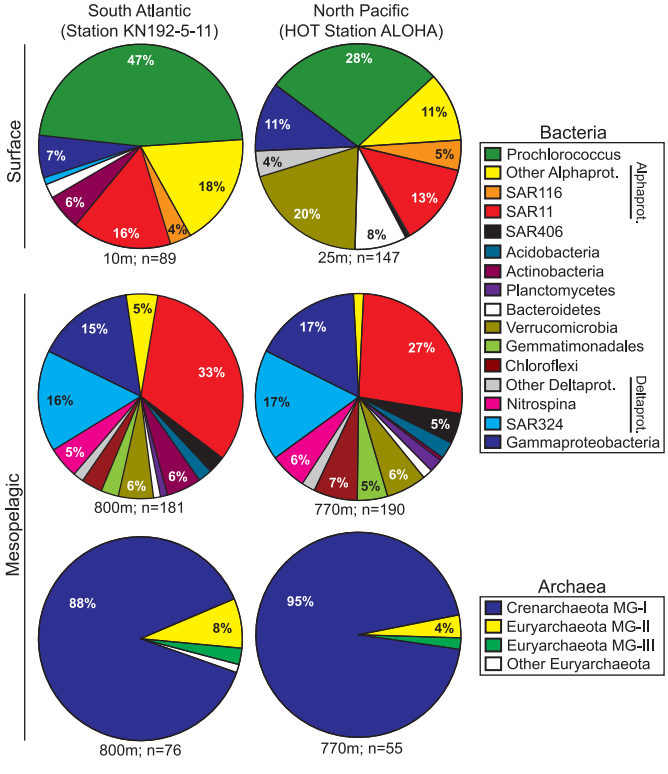

Fig. 1. Proportions of bacterial and archaeal SAGs retrieved from surface and mesopelagic stations, identified by SSU rRNA sequence analysis. Alphaprot., *Alphaproteobacteria*; Deltaprot., *Deltaproteobacteria*.

[1]Bigelow Laboratory for Ocean Sciences, 180 McKown Point Road, Post Office Box 475, West Boothbay Harbor, ME 04575, USA. [2]Monterey Bay Aquarium Research Institute, Moss Landing, CA 95064, USA. [3]Department of Energy Joint Genome Institute, Walnut Creek, CA 94598, USA. [4]Department of Marine Biology, University of Vienna, Faculty Center of Ecology, Althanstrasse 14, A-1090 Vienna, Austria. [5]Department of Biological Engineering and Department of Civil and Environmental Engineering, Massachusetts Institute of Technology, Cambridge, MA 02138, USA.

*Present address: UMR BOREA, CNRS 7208, Muséum National d'Histoire Naturelle, 61 Rue Buffon, 75231 Paris Cedex 5, France.

†To whom correspondence should be addressed. E-mail: rstepanauskas@bigelow.org

that SAR324 cells may be significant contributors to the dark ocean's chemoautotrophy.

RuBisCO sequences similar to those obtained from our SAGs have been detected in other dark ocean regions, including bacterial artificial chromosomes (BACs) from the Monterey Bay OMZ (~700 to 800 m) (figs. S1 and S12 to S14 and tables S3 to S6). The arrangement of the *cbb* operon in BAC clones was similar to that of other RuBisCO operons (*27*), and typical protein active sites and the RuBisCO motif were present in large-subunit sequences (fig. S13). Recently, multiple RuBisCO-containing BAC clones were recovered from aerobic but subphotic depths (200 m) of Monterey Bay (*28*). A time series study of the top 200 m indicates the highest *cbbM* abundance at subphotic depths, and no correlation with the concentration of chlorophyll, indicating decoupling from direct photosynthesis (fig. S15). The high similarity of RuBisCO genes found by this and other studies in various geographic regions suggests that SAR324 cells and *Gammaproteobacteria* represented in our SAG libraries may be the predominant microbial groups encoding these genes in the dark ocean.

To identify potential energy sources for chemoautotrophy in the oxygenated dark ocean, we screened mesopelagic prokaryote SAGs by PCR for genes involved in sulfur, ammonia, and nitrite oxidation (table S1). We recovered *amoA* from the majority of mesopelagic crenarchaeal marine group I SAGs from the South Atlantic (60%) and North Pacific (81%), supporting previous reports that this crenarchaeal group is capable of nitrification (*7*, *9*). Although no ammonia or nitrite oxidation genes were detected in any bacterial SAGs, we found several genes involved in dissimilatory sulfur oxidation (Fig. 2). Sulfur oxidation genes were found only in those bacterial taxonomic groups that also contained RuBisCO, and the same association was found in multiple cells originating from two geographically distant locations. Partial sequences coding for lineage I and II adenosine 5′-phosphosulfate (APS) reductase (*aprA*) were recovered from the *Deltaproteobacteria* SAR324 and *Gammaproteobacteria* lineages ARCTIC96BD-19 and Agg47 (fig. S16A). Lineage I and II *aprA* genes are affiliated with sulfur-oxidizing bacteria (SOB) and are phylogenetically distinguishable from APS reductase involved in sulfate reduction and assimilatory APS pathways (*29*). The *aprA* sequences from *Gammaproteobacteria* SAGs clustered with SOB lineage I, whereas SAR324 *aprA* sequences formed a distinct cluster within SOB lineage II, closely related to *Chlorobi* sequences (fig. S16A). Reverse-type dissimilatory sulfite reductase (*rdsrA*) genes were recovered only from SAR324 SAGs and were most similar to sequences from *Chlorobi* (fig. S16B). The consistent co-occurrence of RuBisCO, *aprA*, and *rdsrA* genes in the same bacterial lineages suggests the potential use of dissimilatory sulfur oxidation for energetic support of autotrophic carbon fixation in these microbes.

Table 1. Summary of bacterial and archaeal SAG PCR screening results.

Station	Depth (m)	Total SAGs*	Identified SAGs†	Metabolic gene screening results‡		
				RuBisCO	*aprA*	*rdsrA*
KN192-5-11	10	311	89 (29%)	ND	ND	ND
	800	1252	257 (21%)	21 (12%)	15 (8%)	1 (0.6%)
ALOHA	25	630	147 (23%)	ND	ND	ND
	770	630	245 (39%)	23 (12%)	17 (9%)	2 (1%)

*Total SAGS are the number with successfully amplified DNA product. †SAGs for which high-quality SSU rRNA sequences were obtained. ‡Percentages based on the total number of identified bacterial SAGs only; ND, no data.

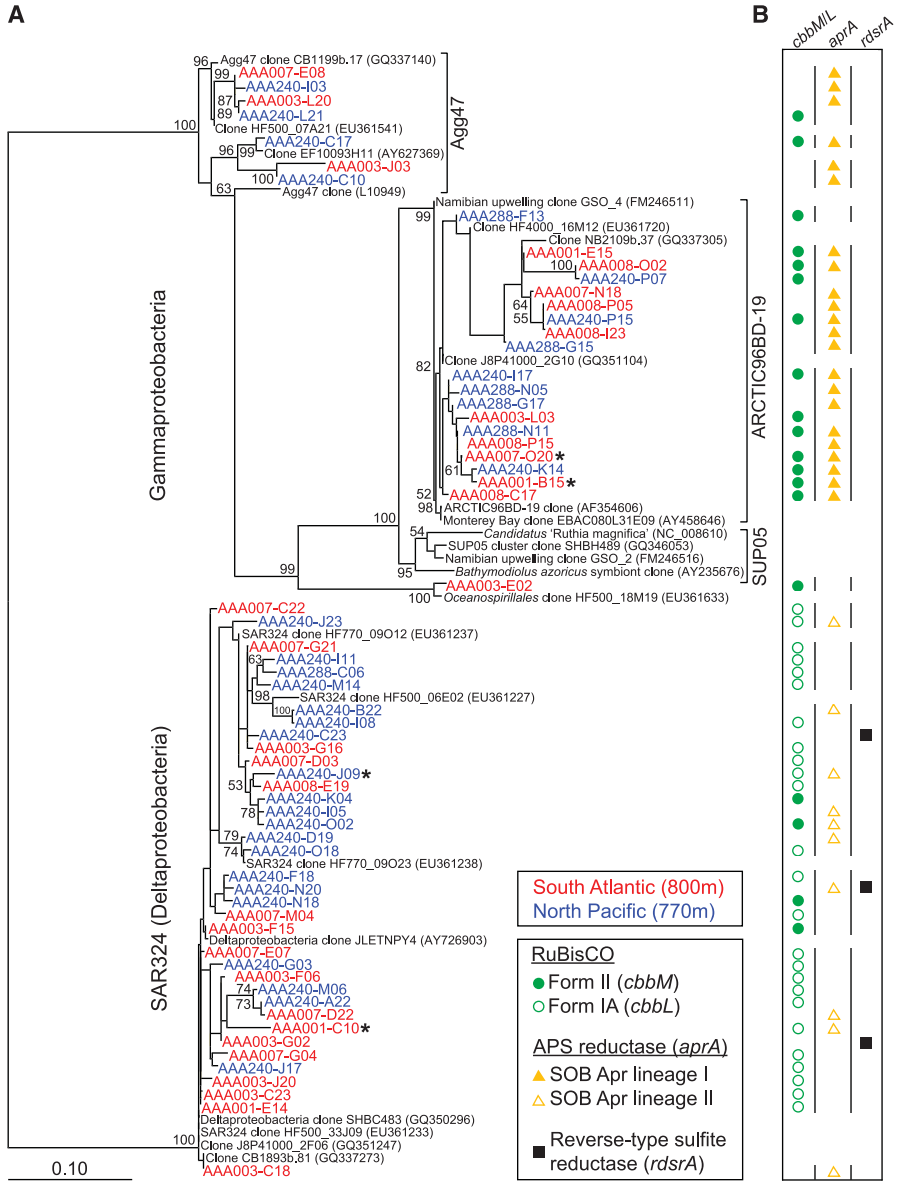

Fig. 2. (**A**) Phylogenetic tree of *Gammaproteobacteria* and *Deltaproteobacteria* SAR324 SSU rRNA sequences of mesopelagic SAGs (in color) recovered from the South Atlantic and North Pacific Subtropical Gyres. SAGs for which draft genomes were generated are marked with asterisks. The tree was inferred using maximum likelihood in the RAxML program. Bootstrap values (1000 replicates) ≥ 50% are indicated at nodes. Displayed are only SAGs in which chemoautotrophy-related genes were detected. (**B**) Occurrence and type of carbon fixation and sulfur oxidation pathway genes recovered from SAGs.

Additional sulfur oxidation genes were identified from whole-genome analysis of ARCTIC96BD-19 and SAR324 SAGs, including genes supporting thiosulfate oxidation, adenosine 5′-triphosphate (ATP) sulfurylase, and sulfate permease (tables S10 to S13). The SAR324 cells also contained genes potentially supporting the oxidation of carbon monoxide and methane and a suite of genes found in methylotrophic pathways (table S14). Together, these data suggest a flexible and opportunistic metabolic lifestyle of the SAR324 lineage.

Because these RuBisCO-containing bacterial lineages are found throughout the dark oxygenated water column (Fig. 3C and fig. S2), it is not immediately apparent what the sources of reduced sulfur compounds are that would be required for chemolithotrophic energy production. Reduced inorganic sulfur is rare outside the vicinity of hydrothermally active or upwelling regions (*2*, *30*). Possible other sources include proteins, osmolytes (such as dimethylsulfoniopropionate), and particles, the hot spots of microbial activity that may contain anoxic microniches (*5*, *31*, *32*). Supporting the latter, we detected a suite of motility and adhesion genes in SAR324 cells (table S15) and confirmed their common association with particles in situ (Fig. 3A). Likewise, Agg47 cells have also been found to be preferentially on particles (*33*). Recently, an active but cryptic sulfur cycle was reported in the OMZ waters off the coast of Chile, where sulfide produced from sulfate reduction is immediately oxidized and therefore does not accumulate in the water column (*4*). The ARCTIC96BD-19 lineage is phylogenetically close to the SUP05 cluster, which dominates many OMZ regions, suggesting the possibility of a similar sulfur dynamic mediated by the former lineage even in well-oxygenated waters.

All four ARTIC96BD-19 and SAR324 genomes possessed multiple ATP-binding cassette (ABC) transporters for sugar transport and accessory periplasmic components, as well as several amino acid and oligopeptide transporters (table S14), often in tandem, indicating co-regulation. This suggests a likely mixotrophic lifestyle for these RuBisCO-containing lineages.

We have demonstrated that several uncultured *Proteobacteria* lineages that are indigenous and abundant in the dark oxygenated ocean are likely mixotrophs and have the potential for autotrophic CO_2 fixation, coupled to the oxidation of reduced sulfur compounds. Some of these dark ocean bacteria may also be methylotrophs, using reduced single-carbon compounds as energy sources for growth. These previously unrecognized metabolic types of dark ocean bacteria may play an important role in global biogeochemical cycles, and their activities may in part reconcile current discrepancies in the dark ocean's carbon budget.

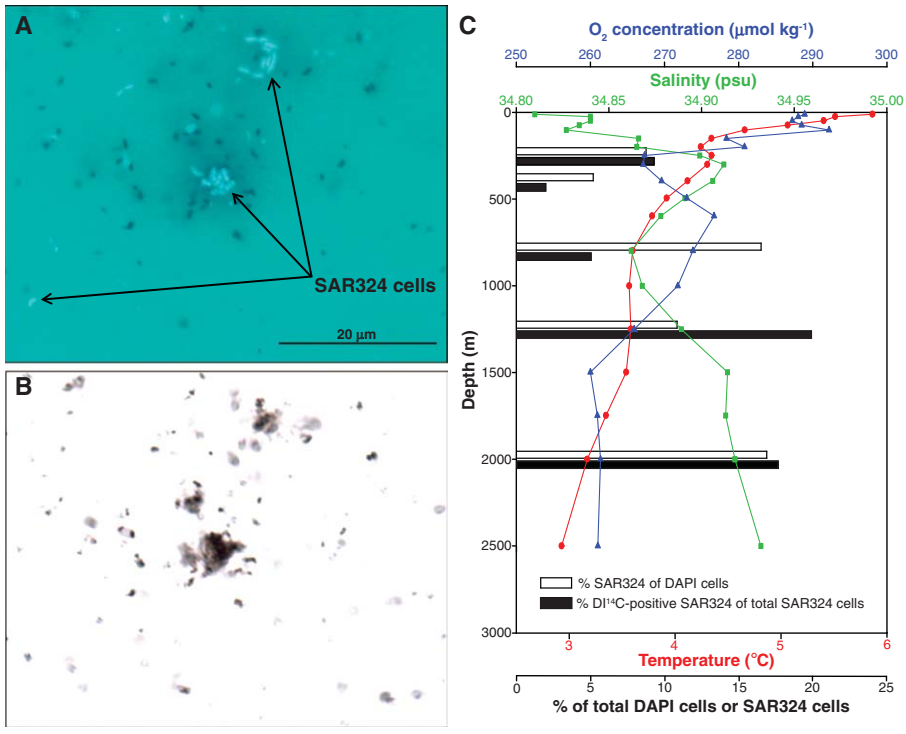

Fig. 3. Micrographs demonstrating bicarbonate uptake and aggregation around particles by *Deltaproteobacteria* SAR324. (**A**) Overlay of transmitted-light and epifluorescence micrographs showing SAR324 cells labeled by CARD-FISH and silver grains indicating bicarbonate uptake by SAR324 (dark gray dots). Particles are also visible (faint grayish background). (**B**) Single-layer transmitted light micrograph for better visibility of the silver halos detected by microautoradiography and particle aggregates. (**C**) Vertical profiles of the percent of SAR324 cells out of total prokaryote cells, the percent of total SAR324 cells positive for dissolved inorganic ^{14}C uptake, temperature, dissolved oxygen, and salinity in the North Atlantic (58.60°N, 39.71°W) during the Dutch Geotraces-1 cruise (RV *Pelagia*, 5 May 2010).

References and Notes

1. P. A. del Giorgio, C. M. Duarte, *Nature* **420**, 379 (2002).
2. D. A. Walsh *et al.*, *Science* **326**, 578 (2009).
3. G. T. Taylor *et al.*, *Limnol. Oceanogr.* **46**, 148 (2001).
4. D. E. Canfield *et al.*, *Science* **330**, 1375 (2010).
5. D. M. Karl, G. A. Knauer, J. H. Martin, B. B. Ward, *Nature* **309**, 54 (1984).
6. T. Reinthaler, H. M. van Aken, G. J. Herndl, *Deep Sea Res. Part II Top. Stud. Oceanogr.* **57**, 1572 (2010).
7. G. J. Herndl *et al.*, *Appl. Environ. Microbiol.* **71**, 2303 (2005).
8. I. A. Berg, D. Kockelkorn, W. Buckel, G. Fuchs, *Science* **318**, 1782 (2007).
9. C. Wuchter *et al.*, *Proc. Natl. Acad. Sci. U.S.A.* **103**, 12317 (2006).
10. H. Agogué, M. Brink, J. Dinasquet, G. J. Herndl, *Nature* **456**, 788 (2008).
11. M. M. Varela, H. M. van Aken, E. Sintes, T. Reinthaler, G. J. Herndl, *Environ. Microbiol.* **13**, 1524 (2011).
12. Materials and methods are available as supporting material on *Science* Online.
13. Y. Marcy *et al.*, *Proc. Natl. Acad. Sci. U.S.A.* **104**, 11889 (2007).
14. A. Raghunathan *et al.*, *Appl. Environ. Microbiol.* **71**, 3342 (2005).
15. R. Stepanauskas, M. E. Sieracki, *Proc. Natl. Acad. Sci. U.S.A.* **104**, 9052 (2007).
16. K. Zhang *et al.*, *Nat. Biotechnol.* **24**, 680 (2006).
17. T. Woyke *et al.*, *PLoS ONE* **4**, e5299 (2009).
18. E. F. DeLong *et al.*, *Science* **311**, 496 (2006).
19. V. D. Pham, K. T. Konstantinidis, T. Palden, E. F. DeLong, *Environ. Microbiol.* **10**, 2313 (2008).
20. J. Arístegui, J. M. Gasol, C. M. Duarte, G. J. Herndl, *Limnol. Oceanogr.* **54**, 1501 (2009).
21. M. T. Suzuki *et al.*, *Microb. Ecol.* **48**, 473 (2004).
22. T. E. Hanson, F. R. Tabita, *Proc. Natl. Acad. Sci. U.S.A.* **98**, 4397 (2001).
23. H. J. Tripp *et al.*, *Nature* **464**, 90 (2010).
24. S. J. Giovannoni *et al.*, *Science* **309**, 1242 (2005).
25. C. M. Turley, P. J. Mackie, *Deep Sea Res. Part I Oceanogr. Res. Pap.* **42**, 1453 (1995).
26. Y. Shi, G. W. Tyson, E. F. DeLong, *Nature* **459**, 266 (2009).
27. N. R. Hayashi, H. Arai, T. Kodama, Y. Igarashi, *Biochem. Biophys. Res. Commun.* **241**, 565 (1997).
28. V. I. Rich, V. D. Pham, J. Eppley, Y. Shi, E. F. DeLong, *Environ. Microbiol.* **13**, 116 (2011).
29. B. Meyer, J. Kuever, *Appl. Environ. Microbiol.* **73**, 7664 (2007).
30. J. Radford-Knoery, C. R. German, J.-L. Charlou, J.-P. Donval, Y. Fouquet, *Limnol. Oceanogr.* **46**, 461 (2001).
31. A. L. Shanks, M. L. Reeder, *Mar. Ecol. Prog. Ser.* **96**, 43 (1993).
32. R. Stocker, J. R. Seymour, A. Samadani, D. E. Hunt, M. F. Polz, *Proc. Natl. Acad. Sci. U.S.A.* **105**, 4209 (2008).
33. E. F. DeLong, D. G. Franks, A. L. Alldredge, *Limnol. Oceanogr.* **38**, 924 (1993).

Acknowledgments: This work was supported by NSF grants EF-826924 and OCE-0821374 (R.S. and M.E.S.), a grant from the Maine Technology Institute (Bigelow Laboratory), U.S. Department of Energy (DOE) JGI 2010 Microbes Program grant CSP77 (R.S. and M.E.S.), the David and Lucille Packard Foundation (C.M.P.), the Gordon and Betty Moore Foundation (E.F.D.), the Dutch Science Fund-Earth and Life Sciences (G.J.H.), the Austrian Science Fund-FWF and European Science Foundation EuroEEFG project MOCA (G.J.H.), and Marie Curie project ARCADIA (G.J.H.). Work conducted by the DOE Joint Genome Institute is supported by the Office of Science of the DOE under contract no. DE-AC02-05CH11231. We thank chief scientist S. Curless, the officers and crew of the RV *Ka'imikai-O-Kanaloa*, and the HOT team for sample collection at station ALOHA; S. Sievert of the Woods Hole Oceanographic Institute for providing PCR primer information; J. Heywood of Bigelow for collecting South Atlantic field samples; the crew of the RV *Point Lobos*; V. Rich for initial screening of Monterey Bay libraries; and F. Chavez, R. Michasaki, and T. Pennington for providing Monterey Bay oceanographic data. SSU rRNA and metabolic gene sequences have been deposited in GenBank with the following accession numbers: SSU rRNA, HQ675122 to HQ675859; *cbbL*, HQ675043 to HQ675069; *cbbM*, HQ675070-HQ675086; *aprA*, HQ675087-HQ675118; and *rdsrA*, HQ675119 to HQ675121. Whole-genome sequence

data have accession numbers AFHZ00000000 (AAA001-B15), AFIB00000000 (AAA001-C10), AFHY00000000 (AAA007-O20), and AFIA00000000 (AAA240-J09). Raw sequences were deposited in the GenBank Short Read Archive under accession numbers SRA029592 and SRA035467 (AAA001-B15), SRA029604 and SRA035394 (AAA001-C10), SRA029593 and SRA035468 (AAA007-O20), and SRA029596 and SRA035470 (AAA240-J09).

Supporting Online Material
www.sciencemag.org/cgi/content/full/333/6047/1296/DC1
Materials and Methods
Figs. S1 to S19
Tables S1 to S15
References

1 February 2011; accepted 13 July 2011
10.1126/science.1203690

Tet Proteins Can Convert 5-Methylcytosine to 5-Formylcytosine and 5-Carboxylcytosine

Shinsuke Ito,[1,2]* Li Shen,[1,2]* Qing Dai,[3] Susan C. Wu,[1,2] Leonard B. Collins,[4] James A. Swenberg,[2,4] Chuan He,[3] Yi Zhang[1,2]†

5-methylcytosine (5mC) in DNA plays an important role in gene expression, genomic imprinting, and suppression of transposable elements. 5mC can be converted to 5-hydroxymethylcytosine (5hmC) by the Tet (ten eleven translocation) proteins. Here, we show that, in addition to 5hmC, the Tet proteins can generate 5-formylcytosine (5fC) and 5-carboxylcytosine (5caC) from 5mC in an enzymatic activity–dependent manner. Furthermore, we reveal the presence of 5fC and 5caC in genomic DNA of mouse embryonic stem cells and mouse organs. The genomic content of 5hmC, 5fC, and 5caC can be increased or reduced through overexpression or depletion of Tet proteins. Thus, we identify two previously unknown cytosine derivatives in genomic DNA as the products of Tet proteins. Our study raises the possibility that DNA demethylation may occur through Tet-catalyzed oxidation followed by decarboxylation.

Although enzymes that catalyze DNA methylation process are well studied (*1*), how DNA demethylation is achieved is less known, especially in animals (*2*, *3*). A repair-based mechanism is used in DNA demethylation in plants, but whether a similar mechanism is also used in mammalian cells is unclear (*3*, *4*). Identification of hydroxymethylcytosine (5hmC) as the sixth base of the mammalian genome (*5*, *6*) and the capacity of Tet (ten eleven translocation) proteins to convert 5-methylcytosine (5mC) to 5hmC in an Fe(II) and alpha-ketoglutarate (α-KG)–dependent oxidation reaction (*6*, *7*) raised the possibility that a Tet-catalyzed reaction might be part of the DNA demethylation process.

A potential 5mC demethylation mechanism can be envisioned from similar chemistry for thymine-to-uracil conversion (*3*, *8*, *9*) (fig. S1A),

[1]Howard Hughes Medical Institute and Department of Biochemistry and Biophysics, University of North Carolina at Chapel Hill, Chapel Hill, NC 27599–7295, USA. [2]Lineberger Comprehensive Cancer Center, University of North Carolina at Chapel Hill, Chapel Hill, NC 27599–7295, USA. [3]Department of Chemistry and Institute for Biophysical Dynamics, University of Chicago, Chicago, IL 60637, USA. [4]Department of Environmental Sciences and Engineering, University of North Carolina at Chapel Hill, Chapel Hill, NC 27599–7295, USA.

*These authors contributed equally to this work.
†To whom correspondence should be addressed. E-mail: yi_zhang@med.unc.edu

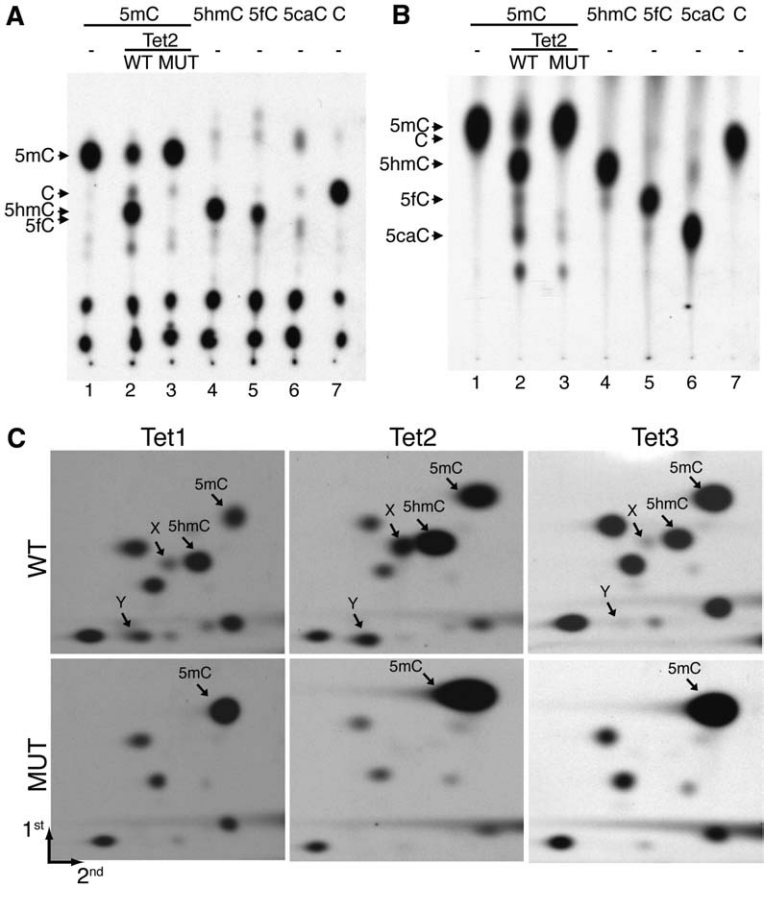

Fig. 1. Optimization of conditions for detection of cytosine and its 5-position modified forms by TLC. (**A**) Migration of labeled C and its 5-position modified forms by TLC under the first developing buffer. Lanes 1 to 3 serve as controls for the migration of 5mC and 5hmC generated from DNA oligos incubated with wild-type (WT) or catalytic mutant (MUT) Tet2. (**B**) The same samples used in (A) were separated by TLC under the second developing buffer. With the exception of 5mC and C, all of the other forms of C can be separated under this condition. (**C**) Autoradiographs of 2D-TLC analysis of samples derived from 5mC-containing TaqI 20-mer oligo DNA incubated with WT and catalytic-deficient mutant Tet1, Tet2, and Tet3.